文章编号：1001-9014(2022)05-0850-06

DOI:10.11972/j.issn.1001-9014.2022.05.008

Relationship between radar reflectivity factor and ice water content of non-spherical cirrus ice crystals at 220 GHz

WANG Biao[1], HUO Yi-Wei[2], GUO Xing[1*], WU Jia-Ji[1]

(1. School of Electronic Engineering, Xidian University, Xi′an 710071, China;
2. Science and Technology on Electromagnetic Scattering Laboratory, Shanghai 200438, China)

Abstract: For the practical needs in the data processing of terahertz radar, the discrete dipole approximation method is used to calculate the backscattering cross-section of non-spherical ice crystals with different shapes. Based on the latest refined ice cloud model, the relationship between the radar reflectivity factor Z_m and ice water content I in 220 GHz is established. The calculation results show that both the shapes of the non-spherical ice crystals and the ice cloud model have a particular influence on the Z_m-I relationship. This study has application value for cloud parameter inversion of mid-latitude cirrus clouds, and it can be helpful for the development of terahertz radar in the detection of clouds.

Key words: cirrus, non-spherical ice crystals, radar reflectivity factor, ice water content, terahertz radar

220 GHz卷云非球形冰晶粒子雷达反射率因子与冰水含量关系研究

王 彪[1], 霍熠炜[2], 郭 兴[1*], 吴家骥[1]

(1. 西安电子科技大学 电子工程学院, 陕西 西安 710071;
2. 电磁散射重点实验室, 上海 200438)

摘要:针对220 GHz太赫兹雷达处理数据的实际需要,应用离散偶极子近似法,计算不同形状非球形冰晶粒子的后向散射截面,并基于最新细化的冰云模型,得到了220 GHz太赫兹波雷达探测的冰水含量I与雷达反射率因子Z_m,建立了Z_m-I关系表达式。计算结果表明,非球形冰晶粒子及冰云模型均对Z_m-I关系有一定的影响。本研究对中纬度卷云的太赫兹波雷达探测的云参数反演有应用价值,并对太赫兹波测云雷达的研制具有借鉴作用。

关 键 词:卷云;非球形冰晶粒子;雷达反射率因子;冰水含量;太赫兹雷达

中图分类号:O451 **文献标识码**:A

Introduction

Cirrus is a critical factor of global radiation balance and is one of the primary sources of uncertainty in satellite inversion and climate model research. The scattering of light by ice crystals not only has effect on the radiation balance of the Earth-atmosphere system but also plays a significant role in the development of many small-scale and even weather-scale precipitation in the middle and high latitudes. Millimeter-wave radars can examine the physical structure, dynamic and small-scale turbulence of clouds, ice water content and recognize ice clouds and water clouds. Cloud radar on CloudSat at 94 GHz can be used to study internal horizontal and vertical structure of cloud[1].

Remote sensing of cloud can be divided into active and passive modes, including microwave radar, microwave radiometer, Lidar et al. The information of cloud top and cloud water path can be obtained by the microwave radiometer. Microwave radar, suitable for detecting cloud particles with a diameter of more than 100 microns, can be utilized to obtain cloud vertical structure

Received date: 2021-09-29, **revised date**: 2021-11-21 **收稿日期**:2021-09-29,**修回日期**:2021-11-21

Foundation items: Supported by the National Natural Science Foundation of China (62005205), Natural Science Foundation of Shanghai (20ZR1455100), Natural Science Basic Research Program of Shaanxi (Program No. 2020JQ-331)

Biography: WANG Biao (1986—), male, Shanghai, senior engineer, master. Research area involves Wave propagation and scattering in random media, E-mail: wangbiao@stu.xidian.edu.cn.

* **Corresponding author**: E-mail: guox@xidian.edu.cn

information. Lidars can detect tiny particles on a micron-scale; however, it can only receive cloud surface information because of its insufficient cloud penetration ability. Terahertz waves lie between the microwave and infrared waves. The terahertz waves are in the Mie scattering region for the large cloud particles, whereas they are in the Rayleigh scattering region for the small cloud particles. As is known, the backscattering of the cloud particles in the Rayleigh scattering region is inversely proportional to the fourth power of the detection wavelength. Thus, the smaller cloud particles have stronger scattering to the terahertz wave. The backscattering of particles in the Mie scattering region is stronger than that in the Rayleigh scattering region. In addition, the study of Hogan at the University of Reading in the United Kingdom shows that low-frequency terahertz waves have great potential for the detection of ice clouds in the atmosphere (mostly 5 to 10 microns in diameter)[2]. Therefore, compared to microwave radar, terahertz radar can detect smaller ice cloud particles, which can be used as a necessary complement to cloud remote sensing.

The terahertz cloud radar utilizes the scattering characteristics of cloud particles on electromagnetic waves. By the analysis of the radar echo the cloud which reflects the macroscopic and microscopic structure of the cloud, we can understand the various characteristics of the cloud. The reflectivity factor values of the cloud can be estimated by measuring the echo intensity, and further, the information of the ice water content and particle size of the cloud. Combined with other observation methods, such as microwave radiometers to measure temperature, humidity, and additional information, more advanced meteorological products can be produced.

In 2012, Leinonen proposed that idealized homogeneous spheroidal models of ice crystals and snowflakes cannot consistently describe radar backscattering from a snowfall when the radar wavelengths are on the order of the snowflake size by analyzing collocated airborne radar measurements at 13.4 GHz, 35.6 GHz and 94 GHz[3]. The accuracy of cloud parameter inversion depends on the accuracy of the measurement and forward model. Therefore, to deal with the data processing requirements of terahertz radar, the scattering characteristics of cirrus ice crystals in terahertz are studied in this work. And further, the model between radar reflectivity factor and ice cloud microphysical parameters is utilized to fit the Z_m-I relational expression. It provides a model for the inversion of cirrus parameters, which can be used as a reference for using terahertz cloud radar.

1 Basic theory

Cirrus clouds, which contain numerous ice crystals with different shapes, belong to the high-rise clouds. The thickness of cirrus clouds ranges from a few hundred meters to 5~7 kilometers, typically 1.5 to 2 kilometers. The horizontal extent ranges from a few kilometers to thousands of kilometers, covering an average of 20%~30% of Earth's sky, which results in a strong influence of the Earth's and atmospheric radiation, and further the weather and climate formation process. The ice cloud model is very complex. The scattering and attenuation characteristics are related to the complex shape and size of the particles and the incident wavelength. The maximum size of the non-spherical ice crystal particles can reach several millimeters. In the accurate radar inversion, it is not enough to treat the ice crystal grains as the Mie scattering ball or ellipsoid. Figure 1 shows six common non-spherical ice crystals[4].

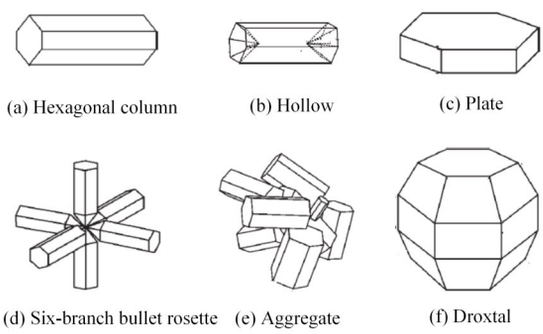

Fig. 1 Ice crystals of different shapes
图1 不同形状的冰晶粒子

Simple shapes of ice crystals can be described by length L and maximum dimensions D. There is an empirical relationship between length L and half width a[5].

1) For a hexagonal column particle of width a, and length L, $L=D$, $a=0.35L$ when $L<100$ μm; when $L>100$ μm, $a=3.48L^{0.5}$.

2) For plate-shaped particles, $L=2.4883a^{0.474}$, $D=2a$, when $a\geqslant 5$ μm.

3) The surface ratio of the bullet rosette particle is related to the length of each branch of the flower pattern. Generally, the particle length and the half-width have a statistical relationship $a=1.552L^{0.63}$, $D=2(L+t)$.

4) Aggregate particles are generally considered to be formed after the polymerization of bullet-type ice crystal grains. The statistical relationship between the half-width a and the particle length L is $a=1.1552L^{0.63}$, $D=7.297L$, and the branch tip of the bullet type particle satisfies the width $t=3^{0.5}/2\tan(\alpha)$, where α represents the inclination to the main axis.

5) Droxtal particles are generally regarded as spherical particles.

The measurement data of cirrus in China is relatively small. In contrast, the measurement of the physical characteristics of mid-latitude and tropical cirrus in foreign countries was carried out earlier, and the data is more comprehensive. At present, the typical measurement data includes FIRE-I, FIRE-II, ARM, TRMM, and CRYSTAL FACE. Field campaigns located in the mid-latitude include the First International Satellite Cloud Climatology Project Regional Experiments in Madison, Wisconsin, in 1986 (FIRE-I) and Coffeyville, Kansas in 1991 (FIRE-II). The distribution of particle size and crystal habit imagery from FIRE-II were obtained from balloon-borne replicators over a size range

Table 1 New feature distribution of cirrus ice crystals
表1 卷云冰晶粒子特征分布

Serial number	Ice crystals	Content (%)	Maximum dimensions(μm)
1	Droxtal	100	D<60
2	Bullet rosette	15	60<D<1 000
	Hexagonal column	50	
	Hexagonal plate	35	
3	Hexagonal column	45	1 000<D<2 500
	Solid hexagonal column	45	
	Aggregate	10	
4	Bullet rosette	97	D>2 500
	Aggregate	3	

from about 10 to 500~1 000 meters. Another mid-latitude dataset was derived in the spring of 2 000 during an Atmospheric Radiation Measurement Program (ARM) intensive observation period near Lamont, Oklahom. In 1998 and 1999, four field campaigns were conducted under the auspices of the Tropical Rainfall Measuring Mission (TRMM). In addition, recent high-quality measurements have been acquired during the Cirrus Regional Study of Tropical Anvils and Cirrus Layers (CRYSTAL) Florida Area Cirrus Experiment (FACE) during a series of flights by the NASA WB57 aircraft and the UND Citation in 2002.

In 2005, after fitting the physical property data in the above five mid-latitude regions and the tropical cirrus database, Baum proposed a new feature distribution of cirrus ice crystals listed in Table 1[6]. The ice crystal habit distribution in the model consists of 100% droxtals when D < 60 mm, 15% bullet rosettes, 50% solid columns, and 35% plates when 60 mm < D < 1 000 mm, 45% hollow columns, 45% solid columns, and 10% aggregates when 1 000 mm < D < 2 500 mm, and 97% bullet rosettes and 3% aggregates when D > 2 500 mm. As shown in Fig. 2, the calculated value agrees well with the actual value, so the feature distribution is applied to calculate the water content and the radar efficiency factor of cirrus in the terahertz band.

Figure 3 shows the particle size distribution of the cirrus particles obtained from the measured data of the mid-latitude cirrus (FIRE-I, FIRE-II, ARM) and tropical cirrus (CRYSTAL, TRMM)[7]. The obtained distribution of different measured data satisfies the gamma distribution $N(D)$ which can be described as[6]

$$N(D) = N_0 D^{\mu} e^{-\beta D} = N_0 D^{\mu} e^{-\frac{b+\mu+0.67}{D_m} D} \quad , \quad (1)$$

where D is the maximum dimensions of ice crystal grains, β is the slope, and μ is the divergence. The liquid ice water content (I) is related to the distribution function[8]

$$I = \rho \int_{D_{min}}^{D_{max}} \left[\sum_{i=1}^{N} f_i(D) V_i(D) \right] N(D) \mathrm{d}(D) \quad , \quad (2)$$

where ρ is ice density, $f_i(D)$ is the habit distribution, of ice crystals, $\sum_{i=1}^{N} f_i(D) = 1$, and $V_i(D)$ is the volume in the case of a given D. The ice water content in the cloud

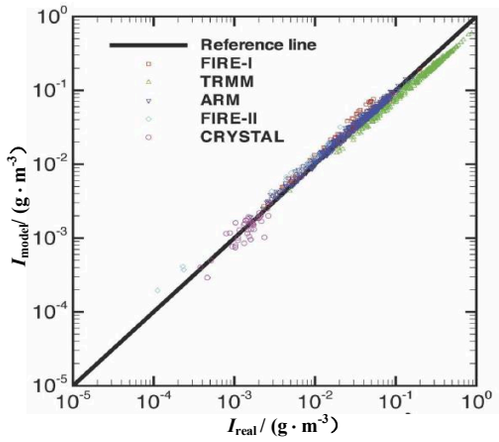

Fig. 2 Comparison of the water content calculated by refined ice cloud model with real values[6]
图2 改进的冰云模型计算的含水量与真实值的对比

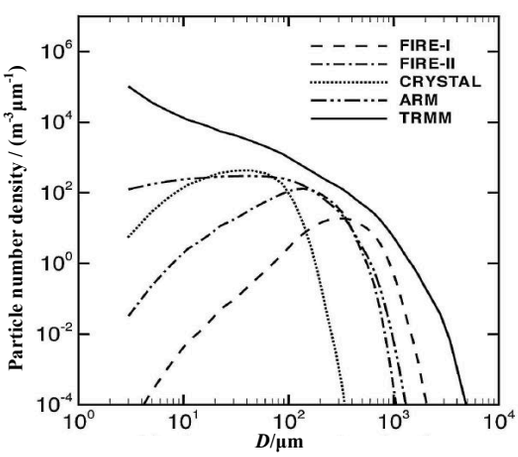

Fig. 3 The measured data of the latitudinal cirrus particle size distribution[6]
图3 中纬度卷云粒度谱分布的实测数据

is calculated from a single ice crystal grain or a mixture of different ice crystal grains. The proportion of different shapes of ice crystals in the cloud can be determined according to the size of D and the ice water content in the ice cloud can be obtained by a weighted average.

The relationship between ice water content I (g/m^3) and D_m and ice crystal spectrum[6] is

$$D_m = \frac{b+\mu+0.67}{\beta} \quad , \quad (3)$$

$$I = \frac{cN_0\Gamma(b+1+\mu)}{\beta^{(b+1+\mu)}} \quad , \quad (4)$$

where N_0, β, and μ are defined by equation (1), c= 6590, b=2.3, and D_m is the median of the droplet spectrum. Different I and D_m can be used to determine different parameters N_0 and β, thus determining different ice crystals.

The radar reflectivity factor is a meteorological parameter related to the distribution of cloud particles. It is

an intrinsic property of the cloud and does not change with detection methods[9]. The properties of the radar reflectivity factor are reflected in its definition. For non-spherical ice crystal particles, the radar reflectivity factor is defined as equation (5). In radar meteorology, the millimeter is usually used as the dimension of the maximum dimensions D of the water droplet, and considering the summation on a unit volume of 1 m^3, the Z unit is usually mm^6/m^3

$$Z_m = \frac{\lambda^4}{\pi^5 |K_i|^2} \int_{D_{min}}^{D_{max}} \left[\sum_{i=1}^{N} f_i(D) \sigma_{ihh}(D) \right] N(D) \mathrm{d}(D), \quad (5)$$

where λ is the incident wavelength, and K_i equals to $(m^2-1)/(m^2+1)$, where m is the complex refractive index of the ice crystal grains. Therefore, if we know the characteristics of the ice cloud (such as the distribution of the cloud droplet spectrum), we can theoretically calculate the radar reflectivity factor value.

The calculation of the backscattering cross-section of non-spherical ice crystals is based on the discrete dipole approximation (DDA) method[10]. It is well-suited for studying the scattering and absorption properties of non-spherical particles, which can be of any shape and heterogeneity. The main principle is to approximate the actual particles with a finite array of discrete and interacting small dipoles that must be sufficient to describe the particles they simulate both in shape and electromagnetic properties; in other words, both of the actual particles and the simulated dipoles have the same discrete relationship. Then, the study of the actual particle scattering properties is transformed into the study of the small dipole scattering properties in these small cubes of side length d. When performing theoretical calculations, the condition $|m|(2\pi/\lambda)d<1$ must be satisfied, m is the complex refractive index of the particles, and λ is the wavelength. The more the value of $|m|(2\pi/\lambda)d$ is smaller than 1, the more accurate the theoretical calculation results are.

2 Results and discussion

The shape and size of the ice crystal were considered in the backscattering section calculation process. The ice cloud model selected in this paper contains six ice crystal grains, and the backscattering sections of the hexagonal column and the hollow hexagonal column are basically the same. Based on the relationship between different ice crystallites L and a, the DDA algorithm was utilized to calculate the backscattering cross- section of six common non-spherical ice crystals shown in Fig. 1.

The temperature was set to 253 K, the frequency was 220 GHz, and the complex refractive index of ice is 1.78+0.0039i. The variation on the backscattering cross section of the ice crystal with the maximum scale in the range of 50~5 000 μm is shown in Fig. 4. It can be seen from the figure that the backscattering cross section of ice crystals with different shapes increases from the increase in the maximum dimension D of the ice crystal grains, and the droxtal contributes more to the backscattering.

In the terahertz radar detection application, it is usually assumed that there is a relationship between the

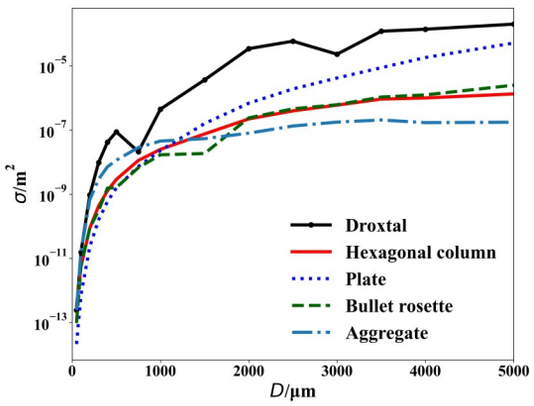

Fig. 4 Variation of backscattering cross section of ice crystals with different shapes of the maximum dimension D
图4 不同形状的冰晶粒子的后向散射截面随冰晶粒子的最大尺度D的变化

ice water content I and the radar reflectivity factor Z_m

$$I = aZ_m^b \quad . \quad (6)$$

The value of N_0 and β can be calculated according to the range of the median D_m and ice water content of ice crystals in the cloud. The range of D_m and I are $0.01 \leqslant D_m \leqslant 0.1$ cm and $10^{-4} \leqslant I \leqslant 10^{-1}$ (g/m^3) respectively. In the above field, 1 000 times (representing 1 000 kinds of ice crystal spectrum distribution were sampled according to the normal distribution D_m: n(0.05, 0.0242) and I: n(0.05, 0.0242)). Then D_m and I were substituted for equation (5) to calculate Z_m in each case. Thus, the Z_m-I relationship of different shapes of ice crystal at 220 GHz was obtained. It can be seen from Fig. 5 that there is a significant difference in the Z_m-I relationship of ice crystals with different shapes. The non-spherical ice crystal grains have a specific influence on the Z_m-I relationship. Treating ice crystal grains as spherical particles cannot fully reflect the Z_m-I relationship.

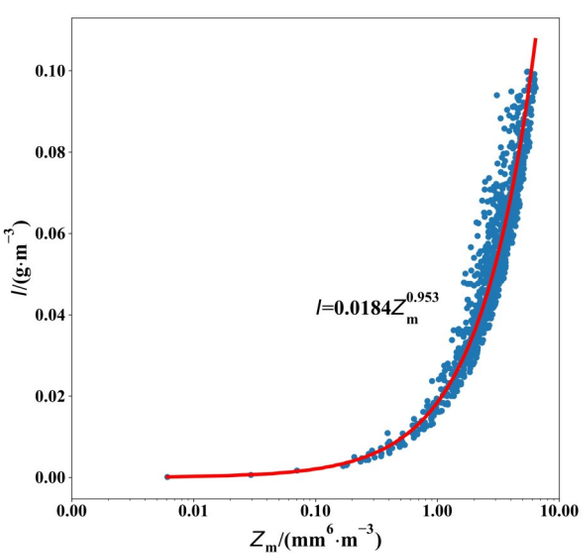

(a)

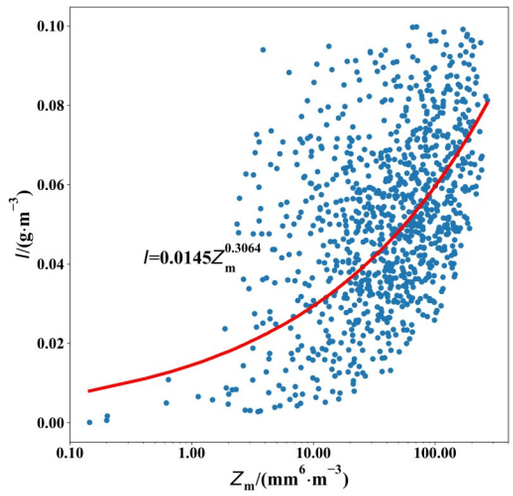

(b)

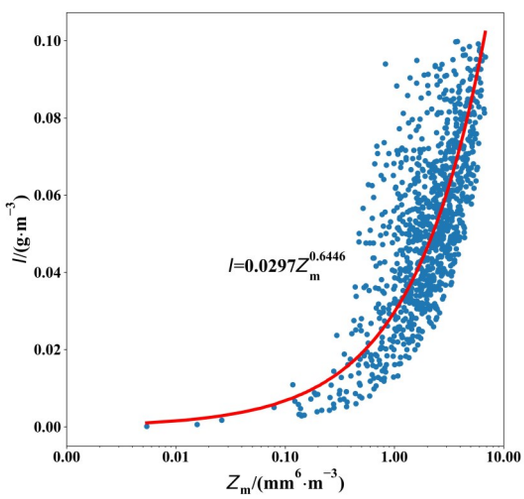

(c)

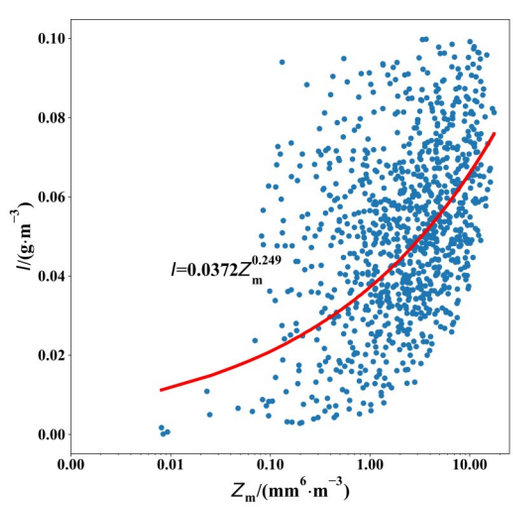

(d)

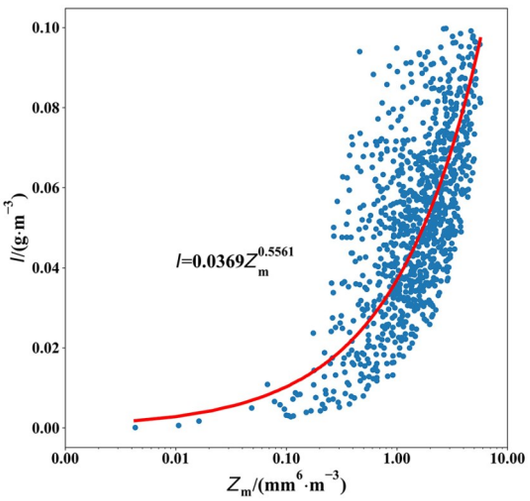

(e)

Fig. 5 Z_m-I relationship of (a) aggregate, (b) droxtal, (c) hexagonal column, (d) plate, (e) bullet rosette
图5 不同形状的冰晶粒子(a) 聚合物, (b) 过冷水滴, (c) 六角空心柱状, (d) 板状, (e) 六瓣子弹花的Zm-I关系

In addition, combined with the ice cloud model provided by Baum et al., the Z_m-I relationship of different shapes of ice crystal particles was calculated. It can be seen from Fig. 6 that the aggregate and the droxtal have little influence on the Z_m-I relationship, whereas the bullet rosette has the most significant effect on it. In addition, the particle size distribution of the ice cloud model has a significant impact on the radar reflectivity factor.

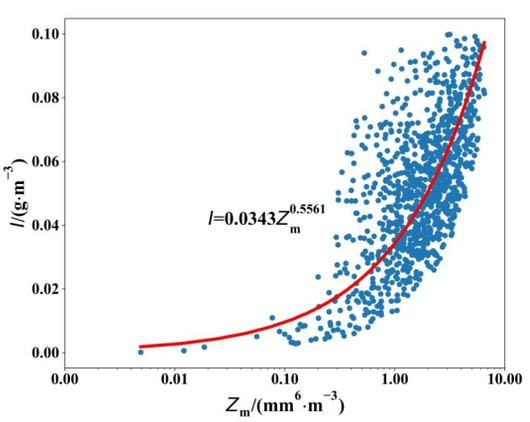

Fig. 6 Zm-I relationship of mixed ice crystal grains
图6 混合冰晶粒子的Zm-I关系

Combined with the same ice cloud model and simulation method, the Z_m-I relationship of different shapes of ice crystal particles was calculated at 94 GHz[7,11-13]. Fig. 7 shows the comparison of the relationships between equivalent radar reflectivity factor Z and ice water content I derived in this study and four other algorithms for ice clouds from previous studies. Atlas and Liu are the measured value, and Teng and Hong are the simulated

values. The present research results are relatively close to the measured value of Atlas and quite different from the simulated values of Teng and Hong. These *Z*m-*I* relationships show pronounced differences. This reveals that the *Z*m-*I* relationship is strongly sensitive to the microphysical properties of ice clouds, such as the ice crystal habits, mixtures of ice crystal habits, and particle size distributions. Obviously, there is no universal *Z*m-*I* relationship to all ice clouds.

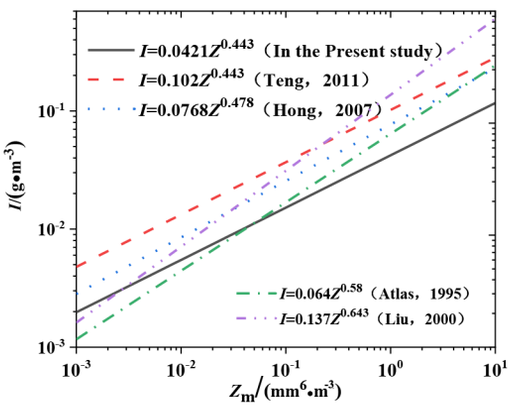

Fig. 7 Comparison of the relationships between *Z*m and *I* derived in this study and other algorithms for ice clouds from previous studies at 94 GHz
图 7 94 GHz 下 Zm-I 之间仿真值与往年研究结果之间的对比

The solid line in Fig. 8 is the fit of the relationship between the radar reflectivity factor and the ice water content obtained by using the EUCREX aircraft to measure the mid-latitude cirrus at 215 GHz for 15 hours[14]. We compare fitted measurements of 215 GHz with the Z_m-*I* relationship model of the 220 GHz mixed ice crystals and spherical particles obtained in this paper. The root mean square error between the measured data and the simulated result of mixed ice crystals and spherical particles are 0. 50 and 0. 57. The correlation coefficient between the measured data and the simulated value of mixed ice crystals and spherical particles are 0. 99 and 0. 95. The source of error is mainly the difference between the parameter selection of the simulation calculation and the natural environment.

3 Conclusions

In this paper, the DDA method was applied to calculate the backscattering cross-section of a single ice crystal with different shapes. Then the Z_m-*I* relation model of different non-spherical ice crystals was obtained by the refined feature distribution model. In this study, we find the *Z*m-*I* relationship is strongly sensitive to the microphysical properties of ice clouds, such as the ice crystal habits, mixtures of ice crystal habits, and particle size distributions. The results show the model with mixed ice crystal particles better fits with experimental data than the single spherical particle model. Later, the characteristic distribution of ice crystals of different heights will be considered to optimize the Z_m-*I* relationship model.

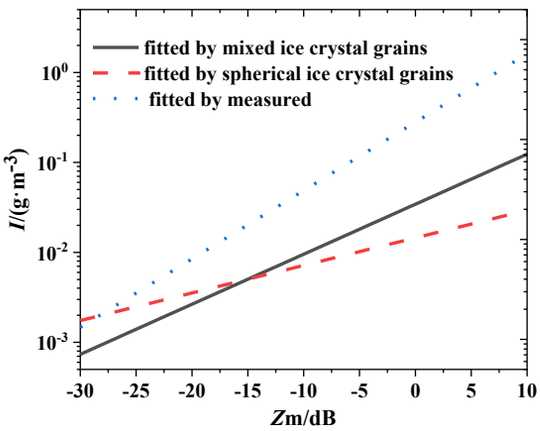

Fig. 8 Comparison of simulated data at 220 GH and measured data at 215 GHz
图 8 220 GHz 下 Zm-I 仿真值与 215 GHz 实测值之间的对比

References

[1] ZHONG Ling-Zhi, LIU Li-Ping and Runsheng G E. Characteristics about the millimeter-wavelength radar and its status and prospect in and abroad [J]. *Advances in Earth Science*, 2009, **24**(4): 383-391.
[2] Hogan R J, Field P R, Illingworth A J, *et al*. Properties of embedded convection in warm-frontal mixed-phase cloud from aircraft and polarimetric radar [J]. *Quarterly Journal of the Royal Meteorological Society*, 2002, **128**(580): 451-476.
[3] Leinonen J, Kneifel S, Moisseev D, *et al*. Evidence of nonspherical behavior in millimeter-wavelength radar observations of snowfall [J]. *Journal of Geophysical Research*, 2012, **117**(D18205).
[4] GANG Hong. Radar backscattering properties of nonspherical ice crystals at 94 GHz [J]. *Journal of Geophysical Research Atmospheres*, 2007, **112**(D22203).
[5] GANG Hong. Parameterization of scattering and absorption properties of nonspherical ice crystals at microwave frequencies [J]. *Journal of Geophysical Research: Atmospheres*, 2007, **112**(D11208).
[6] Baum B A, YANG Ping, Heymsfield Andrew J, *et al*. Bulk Scattering Properties for the Remote Sensing of Ice Clouds. Part II: Narrowband Models [J]. *Journal of Applied Meteorology*, 2005, **44**(12): 1896-1911.
[7] Baum B A, YANG Ping, Heymsfield Andrew J, *et al*. Bulk Scattering Properties for the Remote Sensing of Ice Clouds. Part I: Microphysical Data and Models [J]. *Journal of Applied Meteorology*, 2005, **44**(12): 1885-1895.
[8] GANG Hong, YANG Ping, Baum B A, *et al*. Relationship between ice water content and equivalent radar reflectivity for clouds consisting of nonspherical ice particles [J]. *Journal of Geophysical Research Atmospheres*, 2008, **113**(D20205).
[9] Sato K, Okamoto H. Characterization of Ze and LDR of nonspherical and inhomogeneous ice particles for 95-GHz cloud radar: Its implication to microphysical retrievals [J]. *Journal of Geophysical Research*, 2006, **111**(D22213).
[10] Draine B T, Flatau P J. Discrete-Dipole approximation for scattering calculations [J]. *Journal of the Optical Society of America A*, 1994, **11**(4): 1491-1499.
[11] TENG Xu. Sensitivity of the W band airborne cloud radar reflectivity factor Z to cloud parameters [D]. Nanjing: Nanjing University of information Science and Technology, 2011. (腾煦. 机载 W 波段测云雷达 Z 值对云参数的敏感性研究[D]),南京:南京信息工程大学,2011
[12] Atlas, D, Matrosov Sergey Y, Heymsfield A J, *et al*. Radar and radiation properties of ice clouds, *Journal of applied meteorology*, 1995, **34**(11): 2329-2345.
[13] LIU Chun-Lei, Illingworth Anthony J. Toward more accurate retrievals of ice water Content from radar measurements of clouds, *Journal of applied meteorology*, 2000, **39**(7): 1130-1146
[14] [s.n.] 215 GHz for monitoring ice clouds: Comparison with radar/lidar synergy [R]. Study and Quantification of Synergy Aspects of the ERM. ESTEC Contract 13167/98/NL/GD, [S.l.], 2000.